

The Effects of Nano-anatase TiO₂ on the Activation of Lactate Dehydrogenase from Rat Heart

Yanmei Duan · Huiting Liu · Jinfang Zhao · Chao Liu ·
Zhongrui Li · Jinying Yan · Linglan Ma · Jie Liu ·
Yaning Xie · Jie Ruan · Fashui Hong

Received: 11 December 2008 / Accepted: 19 January 2009 /
Published online: 12 February 2009
© Humana Press Inc. 2009

Abstract Lactate dehydrogenase (LDH, EC1.1.1.27), widely expressed in the heart, liver, and other tissues, plays an important role in glycolysis and glyconeogenesis. The activity of LDH is often altered upon inflammatory responses in animals. Nano-TiO₂ was shown to provoke various inflammatory responses both in rats and mice; however, the molecular mechanism by which TiO₂ exerts its toxicity has not been completely understood. In this report, we investigated the mechanisms of nano-anatase TiO₂ (5 nm) on LDH activity in vitro. Our results showed that LDH activity was greatly increased by low concentration of nano-anatase TiO₂, while it was decreased by high concentration of nano-anatase TiO₂. The spectroscopic assays revealed that the nano-anatase TiO₂ particles were directly bound to LDH with mole ratio of [nano-anatase TiO₂] to [LDH] was 0.12, indicating that each Ti atom was coordinated with five oxygen/nitrogen atoms and a sulfur atoms of amino acid residues with the Ti–O(N) and Ti–S bond lengths of 1.79 and 2.41 Å. We postulated that the bound nano-anatase TiO₂ altered the secondary structure of LDH, created a new metal ion-active site for LDH, and thereby enhanced LDH activity.

Keywords Nano-anatase · TiO₂ · Lactate dehydrogenase · Enzyme kinetics · Conformation

Y. Duan, H. Liu, and J. Zhao contributed equally to this work.

Y. Duan · H. Liu · J. Zhao · C. Liu · J. Yan · L. Ma · J. Liu · J. Ruan · F. Hong (✉)
Medical College of Soochow University, Suzhou 215123, People's Republic of China
e-mail: Hongfsh_cn@sina.com

Z. Li
Nanotechnology Center, University of Arkansas, Little Rock, AR 72204, USA

Y. Xie
Synchrotron Radiation Laboratory, Institute of High Energy Physics, The Chinese Academy of Science,
Beijing 100039, People's Republic of China

Introduction

Advance of nanotechnology has created a variety of nanoparticles. The small size and large surface area endow them with active groups and intrinsic toxicity. Scientists need to address the impact of nanoparticles on human and the environment. Recent studies began to help our understanding in this regard [1–6].

Titanium dioxide (TiO₂), a natural non-silicate mineral oxide, exists in different forms (such as anatase, rutile, and brookite) and is being widely used in the cosmetics, pharmaceutical, and paint industries owing to its high stability, anticorrosion, and photocatalysis [7]. It is well known that lactate dehydrogenase (LDH, EC1.1.1.27) is an important isoenzyme in glycolysis and glyconeogenesis, widely existing in the heart, liver, lung, and many other tissues. When the tissues are subjected to injury, LDH would leak into the serum of blood from the organs or cells, resulting in the increase in LDH activity and its isoenzyme in the corresponding organs [8]. TiO₂ has been shown to cause lung pathogenesis and accumulation of bronchoalveolar lavage fluid (BALF) in mice, rats, and hamsters using bronchial instillation and inhalation methods [8–14]. Bronchial injection of nano-TiO₂ (<30 nm) to rats not only increased the number of alveolar macrophage but also the activities of glutathione peroxidase, glutathione reductase, 6-phosphate glucose dehydrogenase, and glutathione S-transferase as well [15]. However, the enhancement of the enzyme activities did not appear to curb the production of lipid peroxidation and hydrogen peroxide radicals [15], indicating that nano-TiO₂ could induce cells to produce antioxidant enzymes by a mechanism of self-protection. Twenty-nanometer nano-TiO₂ but not 250-nm TiO₂ particles caused pulmonary inflammatory responses in rats and mice and induced the production of the total protein of BALF and the activities of acid-glucosidase and LDH and glyconeogenesis [16]. Nano-TiO₂ particles of 25, 80, and 5 nm increased the ratio of alanine aminotransferase to aspartate aminotransferase, the activity of LDH, and the liver weight, and caused the hepatocyte necrosis in adult mice [17,18]. These studies demonstrated the toxicity of nano-TiO₂; however, its molecular mechanism remains poorly understood.

The aim of this work was to study the effect of nano-anatase TiO₂ (5 nm) on the LDH activity *in vitro*. We report in this paper that nano-anatase TiO₂ could directly bind LDH, alter its secondary structure, and thereby enhance its enzymatic activity.

Material and Methods

Material Treatment

LDH (origin of rat heart) was purchased from Amresco Co. 2-[4-(2-Hydroxyethyl)-1-piperazinyl]ethanesulfonic (HEPS), NADH, and sodium pyruvate were purchased from Sigma Co. Nano-anatase TiO₂ was prepared via controlled hydrolysis of titanium tetrabutoxide. The details of the synthesis are as follows [19]: Colloidal titanium dioxide was prepared via controlled hydrolysis of titanium tetrabutoxide. In a typical experiment, 1 ml of Ti(OC₄H₉)₄ dissolved in 20 ml of anhydrous isopropanol was added dropwise to 50 ml of double-distilled water and adjusted to pH 1.5 with nitric acid under vigorous stirring at room temperature. Then, the temperature was raised to 60°C and kept 6 h for better crystallization of nano-TiO₂ particles. The resulting translucent colloidal suspension was evaporated by using a rotary evaporator, which yields nanocrystalline powder. The obtained powder was washed three times with isopropanol and dried at 50°C until complete

evaporation of the solvent. The average grain size calculated from broadening of the (101) XRD peak of anatase using Scherrer's equation was approximately 5 nm. The Ti^{4+} content in the nano-anatase was measured by inductively coupled plasma mass spectrometry (ICP-MS), and O, C, and H contents in the nano-anatase were assayed by Elementar Analysensysteme GmbH, showing that Ti, O, C, and H contents in the nano-anatase were 58.114%, 40.683%, 0.232%, and 0.136% in nano-anatase compositions, respectively.

LDH Activity Assay

A 0.1-mM HEPS (pH 7.4) buffer was used as a suspending agent. Nano- TiO_2 powder was dispersed onto the surface of HEPS (pH 7.4) buffer, and then the suspending solutions containing nano- TiO_2 particles were treated by ultrasonic for 30 min and mechanically vibrated for 5 min. On the basis of preliminary experiments, the mole ratios of $[\text{TiO}_2]$ to $[\text{LDH}]$ were 0, 0.015, 0.03, 0.045, 0.06, 0.08, 0.12, 0.16, 0.2, 0.24, 0.32, and 0.36, respectively. The activity of LDH was assayed by monitoring its ability to oxidize NADH [20]. Various concentrations of nano-anatase particles were incubated with 50 μM LDH, and 3 ml of reaction mixture containing 0.1 mM HEPS (pH 7.4), 2.3 μM sodium pyruvate, 0.53 μM NADH, and 10 μl of the enzyme was used to monitor the change of absorbance at 340 nm following the addition of the NADH. One unit of enzyme activity was defined as a decrease in absorbance of 0.001 min^{-1} at 340 nm.

Absorption and Fluorescence Spectra Assay of LDH

Various concentrations of nano- TiO_2 particles were incubated with 50 μM LDH and 3 ml of reaction mixture containing 0.1 mM HEPS (pH 7.4). The mole ratios of $[\text{TiO}_2]$ to $[\text{LDH}]$ were 0, 0.015, 0.03, 0.045, 0.06, 0.08, 0.12, 0.16, 0.2, and 0.24.

The optical absorption spectrum of the LDH treated by nano-anatase TiO_2 was measured from 200 to 340 nm at room temperature with a dual-beam spectrophotometer (UV-3010, Hitachi Co., Japan).

Fluorescence measurements were performed on a Hitachi spectrofluorometer Model F-4500 equipped with a 150-W xenon lamp and slit width of 5 nm. A 1-cm quartz cell was used for these studies. The fluorescence spectrum of LDH treated by nano- TiO_2 was recorded at 273 K in the range from 280 to 400 nm upon excitation at 280 nm.

Assay of EXAFS Spectroscopy

In order to detect the local coordination environment at Ti sites, Ti K-edge X-ray absorption data of the nano- TiO_2 -treated LDH (the mole ratio of $[\text{TiO}_2]/[\text{LDH}]$ was 0.12) after being cryodesiccated to powder were collected in fluorescence mode under liquid nitrogen temperature at the 4W1B beamline of the Beijing Synchrotron Radiation Facility (operating at dedicated mode of 2.2 GeV and 40–80 mA). A Ge(111) double-crystal monochromator was used and detuned to minimize the higher harmonic contamination at high energy region. Energies were calibrated using an internal corresponding Ti foil standard. The biological samples were placed in a cuvette and sealed with Kapton tape as transmission windows. A Lytle fluorescence detector was utilized with a Cr filter. More than five scans were recorded and averaged in order to improve the signal-to-noise ratio. For a given sample, no photon reduction should be observed in the first collected spectra compared with the last. The first inflection for edge of the corresponding metal foil was used for energy calibration.

The extended X-ray absorption fine structure (EXAFS) data were extracted from the absorption spectra obtained by averaging the raw data collected over five consecutive scans and normalized by dividing the absorption spectra by the height of the edge jump. Background removal was performed by following standard procedure. The absorption threshold for a core electron excitation was selected at the inflection point in the rise of the “white-line” absorption peak. Correlations between (E_0 , δr_j) and (N_j , σ_j^2) fitting parameters were reduced by weighting the XAFS data by k^n ($n=1, 2, 3$). The passive electron amplitude reduction factor (S_0^2), which is assumed to depend only on the absorbing atom type and not on its environment, was obtained from its fits to those corresponding metal foil data collected under the same condition and set to this value in all other fits. The structural parameters were obtained by curve-fitting the experimental data with the theoretical functions by nonlinear least squares minimization of the residuals. The data were analyzed using the EXAFSPAK analysis suite (<http://www-ssrl.slac.stanford.edu/~george/exafspak/exafs.htm>) together with theoretical standards from the FEFF code, and the latter was used to calculate amplitude and phase shift functions [21].

CD Spectra of LDH

Circular dichroism (CD) spectra were detected at room temperature on a Jasco-J-810 spectropolarimeter with a quartz sample cell of an optical path length of 1 cm. The concentration of LDH treated by various concentrations of nano-anatase TiO₂ was 0.3 mg·mL⁻¹. The mole ratios of [TiO₂] to [LDH] were 0, 0.015, 0.03, 0.045, 0.06, 0.08, 0.12, 0.16, 0.2, 0.24, 0.32, and 0.36. Molecular ellipticities [θ] in deg·cm²·dmol⁻¹ were calculated using a mean residue weight of 115. The secondary structure indices (α -helix, β -sheet, β -turn, and random coil) of the enzyme samples were determined by using Perczel's method [22]. The method, called “convex constraint analysis,” is a general deconvolution method for a CD spectra set of any variety of conformational type. The algorithm, based on a set of three constraints, is able to deconvolute a set of CD curves to its common “pure” component curves and conformational weights. To analyze a single CD spectrum obtained by this method, the spectrum is appended to the data set used as a reference data set.

Statistical Analysis

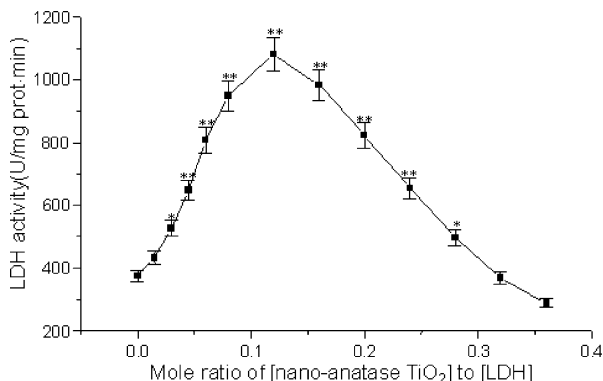
The assay mentioned above was replicated five times. All data were expressed as mean \pm standard error and were analyzed by an analysis of variance (ANOVA). If significance was found in ANOVA, group means were compared using Student's *t* test. Differences were considered significant when $p \leq 0.05$.

Result and Discussion

Activation of Nano-anatase TiO₂ on LDH

The in vitro LDH activity assays were carried out to investigate the interaction between LDH and nano-TiO₂. LDH activity was increased rapidly when the size of mol ratios of [TiO₂] to [LDH] from 0.015 to 0.12 ($P < 0.05$ or 0.01), while for the size of mole ratios of [TiO₂] to [LDH] from 0.16 to 0.36, the LDH activity decreased slowly ($P < 0.05$ or 0.01; Fig. 1). Some researches indicated that nanoparticles could significantly increase LDH activity in rats and mice [16–18, 23]. According to Fig. 1, we also assayed the kinetics

Fig. 1 Effects of nano-anatase TiO_2 on the LDH activity of rat heart. The activity of LDH was assayed by monitoring its ability to oxidize NADH. One unit of enzyme activity was defined as a decrease in absorbance of 0.001 min^{-1} at 340 nm. Data values are mean \pm SE of five experimental replicates ($n=5$). Dots marked with an asterisk and double asterisks were different from the control ($[\text{TiO}_2]/[\text{LDH}]=0$) at the 5% confidence level and at the 1% confidence level, respectively

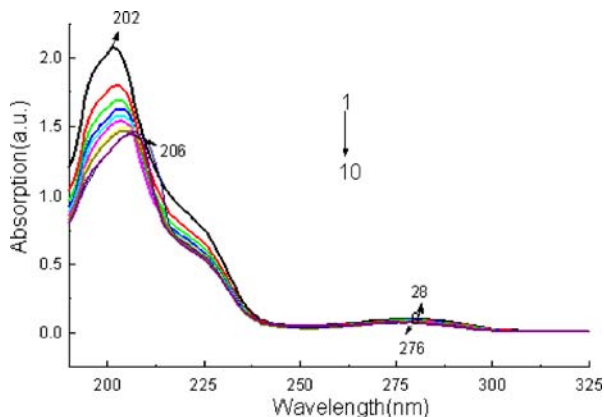


constant (K_m) and V_{\max} of LDH, suggesting that K_m and V_{\max} were $6 \times 10^{-3} \mu\text{M}$ and $11,490 \text{ mg}^{-1} \text{ protein} \cdot \text{min}^{-1}$, respectively, and $3.1 \times 10^{-2} \mu\text{M}$ and $221 \text{ U} \cdot \text{mg}^{-1} \text{ protein} \cdot \text{min}^{-1}$, respectively. It was determined that LDH had a stronger affinity for nano- TiO_2 when nano- TiO_2 was at a low concentration; however, the affinity of LDH for nano- TiO_2 conspicuously declined when nano- TiO_2 was at a high concentration.

Coordination of Nano-anatase TiO_2 on LDH

UV absorption spectra of LDH were generated with various concentrations of nano- TiO_2 (Fig. 2). The spectra exhibited two absorption peaks at 202 and 280 nm, which are the characteristic peaks of $\pi \rightarrow \pi^*$ electron transition of the acid amide bonds or cysteine or peptide chain skeleton, and tryptophan/tyrosine structures, respectively. Two characteristic peaks of LDH were red shifted by 2–4 nm and blue shifted (Soret band) by 2–4 nm, respectively, and the peak intensities of LDH were decreased with the addition of nano- TiO_2 ; the reduction of amide bond or cysteine peak was lower than that of tryptophan/tyrosine peak (Fig. 2). These results suggest that nano- TiO_2 might primarily coordinate with O or N of tryptophan/tyrosine and then coordinate with S of cysteine of LDH protein. The red shift of peptide chain skeleton indicated that it was exposed to polar environment more, e.g., the peptide chain stretch. The blue shift of Soret band suggested that the hydrophobic

Fig. 2 Effect of nano-anatase TiO_2 on the UV absorption of LDH of rat heart. The concentration of the nano-anatase TiO_2 -treated LDH was $0.1 \text{ mg} \cdot \text{mL}^{-1}$.
 1 $[\text{TiO}_2]/[\text{LDH}]=0$;
 2 $[\text{TiO}_2]/[\text{LDH}]=0.015$;
 3 $[\text{TiO}_2]/[\text{LDH}]=0.03$;
 4 $[\text{TiO}_2]/[\text{LDH}]=0.045$;
 5 $[\text{TiO}_2]/[\text{LDH}]=0.06$;
 6 $[\text{TiO}_2]/[\text{LDH}]=0.08$;
 7 $[\text{TiO}_2]/[\text{LDH}]=0.12$;
 8 $[\text{TiO}_2]/[\text{LDH}]=0.16$;
 9 $[\text{TiO}_2]/[\text{LDH}]=0.2$;
 10 $[\text{TiO}_2]/[\text{LDH}]=0.24$



of tryptophan or tyrosine residues increased. The reduction of absorbance corresponds to the reduced probability of $\pi \rightarrow \pi^*$ electron transition because the exposure degree of O of tryptophan/tyrosine of LDH reduced and the space resistance increased.

The effect of nano-TiO₂ on LDH was evaluated by measuring the intrinsic fluorescence intensity of the LDH–nano-TiO₂ complex. As shown in Fig. 3, the fluorescence emission peak of the control of LDH was 351 nm, which is attributed to tryptophan (Trp). With the increase in nano-TiO₂ concentration, the emission peak was blue shifted, suggesting that nano-TiO₂ made the fluorescent chromophores (Trp) of LDH exposed to the hydrophobic environment. When the ratios of [TiO₂] to [LDH] were between 0.12 and 0.2, the emission peak almost had no change, suggesting the existence of a stable intermediate of partial folding, consistent with the above UV absorbance. The fluorescence intensity was also found to decrease gradually with the addition of nano-TiO₂, which strongly suggests that nano-TiO₂ bind to the LDH protein, leading to the reduction of Trp residue exposure. However, the reduction of fluorescence intensity was not obvious at a high concentration of nano-TiO₂, suggesting that the binding sites for nano-TiO₂ on the LDH protein were already saturated, and the saturation was completed at the mole ratio of 0.12 ([TiO₂]/[LDH]=0.12). The turning point of quenching effect was accorded with the highest point of the LDH activity (Fig. 1).

EXAFS Spectra of Nano-anatase TiO₂–LDH

X-ray absorption spectroscopy (XAS) has been proven to be a very powerful technique to probe the local structure around specific elements. The EXAFS contains information of local atomic arrangement for each absorber atom, as described in the theoretical formula based on the single scattering contribution to XAFS. The X-ray fluorescence excitation XAS warrants detection of low concentrations of transition metals present in metalloenzyme and DNA systems [24].

In order to investigate the direct effects of Ti on LDH, we employed X-ray absorption technique to study the coordination structure at Ti sites in nano-anatase TiO₂–LDH ([TiO₂]/[LDH]=0.12). K edge of Ti⁴⁺ in nano-TiO₂–LDH complex is shown in raw absorption spectrum (Fig. 4), which presents the characteristic of the strong Ti⁴⁺ white line. The Fourier transform for the κ^3 -weighted Ti K-edge EXAFS oscillations in the range of 1–6 Å and the scattering path contributions obtained from curve fittings are shown in

Fig. 3 Effect of nano-anatase TiO₂ on the fluorescence emission spectra of LDH in the rat heart. The concentration of the nano-anatase TiO₂-treated LDH was 0.1 mg·mL⁻¹.

- 1 [TiO₂]/[LDH]=0;
- 2 [TiO₂]/[LDH]=0.015;
- 3 [TiO₂]/[LDH]=0.03;
- 4 [TiO₂]/[LDH]=0.045;
- 5 [TiO₂]/[LDH]=0.06;
- 6 [TiO₂]/[LDH]=0.08;
- 7 [TiO₂]/[LDH]=0.12;
- 8 [TiO₂]/[LDH]=0.16;
- 9 [TiO₂]/[LDH]=0.2;
- 10 [TiO₂]/[LDH]=0.24

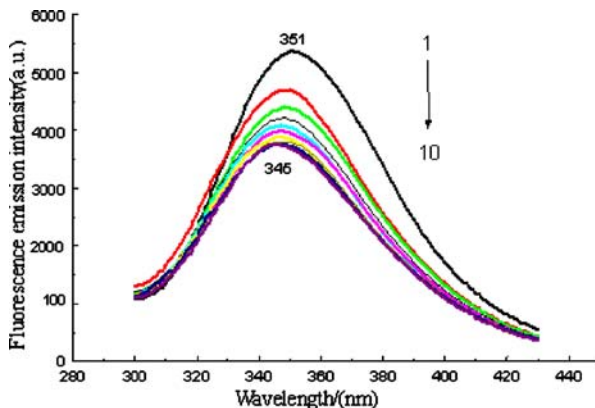


Fig. 4 Fluorescence extended X-ray absorption fine structure spectrum of Ti^{4+} in LDH of rat heart. Ti K-edge X-ray absorption data of LDH from the nano-anatase TiO_2 -treated SOD $[\text{TiO}_2]/[\text{LDH}] = 0.12$ were collected in fluorescence mode under liquid nitrogen temperature

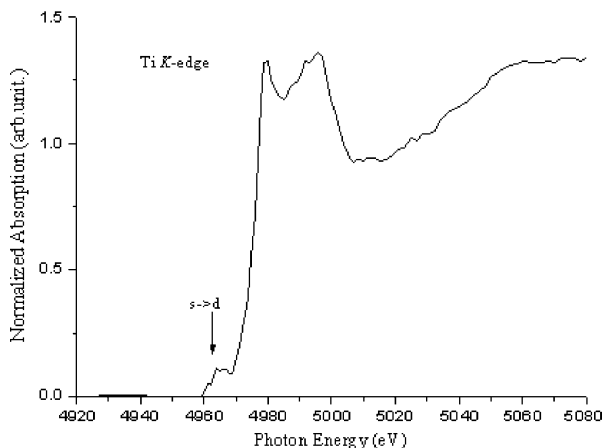


Fig. 5. The local structure coordination parameters obtained from the curve fitting are listed in Table 1, showing that Ti is bound with five oxygen or nitrogen atoms on LDH in its first shell at the distance of the Ti–O (N) bond of 1.79 Å. The second shell at 2.41 Å is a sulfur (S) atom. Taken together, our data showed that nano-anatase TiO_2 might be bound with the oxygen (nitrogen) atoms of amino acid residues (such as Trp) or the sulfur atom of sulfhydryl group (such as Cys) in LDH.

Secondary Structure of LDH

To further confirm that nano- TiO_2 treatment might affect the secondary structure of LDH, the CD spectra of the enzyme were generated with various concentrations of nano- TiO_2 in the reactions. The CD spectrum of LDH had negative cotton peaks at 208 and 220 nm, while the CD spectra of LDH treated with various concentrations of nano- TiO_2 difference showed marked difference. Analysis using Perczel's method indicated that the α -helix

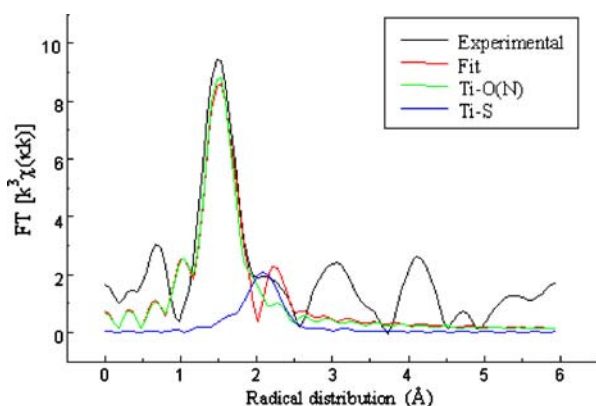


Fig. 5 Radical distribution function Ti^{4+} in LDH of rat heart. Radical distribution function (Fourier transforms of κ^3 -weighted EXAFS oscillation $\chi(\kappa)$) of Ti^{4+} in LDH from rat heart. The experimental curve (black line) is compared with the fitting result (red line). The nonlinear least-square curve fitting revealed that Ti is bound with five oxygen or nitrogen atoms on LDH in its first shell (green) at the distance of the Ti–O (N) bond of 1.79 Å. The second shell (blue) around 2.41 Å is a sulfur (S) atom (for interpretation of the references to color in this figure legend, the reader is referred to the web version of this paper)

Table 1 The Coordination Parameters Obtained from Curve Fitting of EXAFS

Sample	Shell	<i>N</i>	<i>R</i> (Å)	(\AA^2)	<i>E</i> ₀ (eV)
Fresh	Ti–N/O	5	1.79	0.0037	1.5
	Ti–S	1	2.41	0.0051	

The errors of data and fits are roughly estimated from the changed of the residual factors to be 5% for *N*, 0.25% for *R*, 10% for σ^2 , and 4 eV for ΔE_0 . No ambiguities of the theoretical standards are included. Shell indicates the type of ligands for each shell of the fit. *N* is the coordination number. *R* is the metal-scatterer distance. Superscripted 2 is the mean square deviation in *R*. *E*₀ is the shift in *E*₀ for the theoretical scattering functions. Numbers in parentheses were not varied during optimization

contents of LDH treated with the mole ratios of [TiO₂] to [LDH] from 0 to 0.12 were gradually increased and then declined gradually, consistent with the increase or decrease of the enzyme activity (Table 2 and Fig. 1). Since the changes of β -sheet, random coil, and β -turn of LDH are random, the changes of LDH activities observed would point to the α -helix changes of LDH secondary structure. This result further confirms that the enzyme activity is directly related to α -helix of secondary structure [25].

Conclusion

In this study, we showed that LDH activity was greatly increased by low concentrations of nano-anatase TiO₂, while it was decreased by high concentrations of nano-anatase TiO₂. The spectroscopic assays demonstrated that the nano-TiO₂ directly binds to LDH, and the mole ratio of binding of [TiO₂] to [LDH] was 0.12, i.e., five oxygen or nitrogen atoms and

Table 2 LDH Secondary Structure by Nano-anatase TiO₂ Treatments

Mole ratio of [TiO ₂]/[LDH]	α -helix (%)	β -sheet (%)	Random coil (%)	β -turn (%)
0	32.90±1.65	21.77±1.09	29.89±1.49	15.55±0.78
0.015	34.30±1.72	12.84±0.64 ^b	28.30±1.42	22.77±1.14 ^a
0.03	37.714±1.89 ^a	12.24±0.61 ^b	27.59±1.38	18.96±0.95
0.045	38.82±1.94 ^a	13.44±0.67 ^b	28.49±1.42	19.46±0.97
0.06	39.02±1.95 ^a	14.04±0.70 ^b	17.25±0.86 ^a	29.89±1.49 ^b
0.08	39.32±1.97 ^a	16.75±0.84 ^a	15.65±0.78 ^b	28.59±1.43 ^b
0.12	43.13±2.16 ^b	13.24±0.66 ^b	18.46±0.92 ^a	28.18±1.41 ^b
0.16	38.11±1.91 ^a	13.04±0.65 ^b	30.09±1.51	19.06±0.95
0.20	35.81±1.79	7.22±0.36 ^b	26.08±1.30	25.38±1.27 ^b
0.24	35.11±1.76	10.43±0.52 ^b	25.68±1.28	18.96±0.95
0.28	34.90±1.75	13.14±0.66 ^b	28.08±1.40	22.17±1.11 ^a
0.32	33.80±1.69	14.24±0.71 ^b	28.39±1.42	19.16±0.96
0.36	33.40±1.67	17.65±0.88 ^a	29.19±1.46	18.25±0.91

The secondary structure indexes, α -helix, β -sheet, random coil, β -turn of the enzyme samples were determined by Perczel's methods [22]. Data values are mean±SE of five experimental replicates (*n*=5)

^a Different from the control ([TiO₂]/[LDH]=0) at the 5% confidence level

^b Different from the control ([TiO₂]/[LDH]=0) at the 1% confidence level

a sulfur atom of amino acid residues at the Ti–O(N) and Ti–S bond lengths of 1.79 and 2.41 Å, respectively. The binding of nano-TiO₂ altered the secondary structure of LDH. Therefore, we hypothesize that nano-anatase TiO₂ coordination created a new metal ion-active site in LDH, resulting in an enhancement of LDH activity

Acknowledgments This work was supported by the National Natural Science Foundation of China (grant no. 20671067) and by the Medical Development Foundation of Suzhou University (grant no. EE120701) and by the National New Ideas Foundation of Student (grant no. 57315427).

References

1. Service R F (2003) American Chemical Society meeting: nanomaterials show signs of toxicity. *Sci* 300: 243.
2. Brumfiel G A (2003) Little knowledge. *Nature* 424(17): 246.
3. Zhang W X (2003) Environmental technologies at the nanoscale. *Environ Sci Technol* 37(5): 103–108.
4. Kelly K L (2004) Nanotechnology grows up. *Sci* 304: 1732–1734.
5. Sayes, C.M., Wahi, R., Kurian, P.A., Liu, Y.P., West, J.L., Ausman, K.D., Warheit, D.B., Colvin V.L., 2006 Correlating nanoscale titania structure with toxicity: a cytotoxicity and inflammatory response study with human dermal fibroblasts and human lung epithelial cells. *Toxicol Sci* 92, 174–185.
6. Wang B, Feng WY, Zhao Y L, Xing G M, Chai ZF, Wang HF, Jia G (2005) Status of study on biological and toxicological effects of nanoscale materials. *Sci China, Ser B* 48(5): 385–394.
7. Crabtree R H (1998) A new type of hydrogen bond. *Sci* 282: 2000–2001.
8. Wang J Y, Zhu S G, Xu C F ed. (2002) *Biochemistry*. Higher Education Press, Beijing, pp. 356,362, 428 (in Chin).
9. Bermudez E, Mangum JB, Wong BA, Asgharian B, Hext PM, Warheit DB, Everitt JI (2004) Pulmonary responses of mice, rats, and hamsters to subchronic inhalation of ultrafine titanium dioxide particles. *Toxicol Sci* 77: 347–357.
10. Bermudez E, Mangum JB, Asgharian B, Wong BA, Reverdy E, Janszen DB, Hext PM, Warheit DB, Everitt JI (2002) Long-term pulmonary responses of three laboratory rodent species to subchronic inhalation of pigmentary titanium dioxide particles. *Toxicol Sci* 70: 86–97.
11. Driscoll KE, Lindenschmidt RC, Maure JK, Higgins JM, Ridder G (1990) Pulmonary response to silica or titanium dioxide: inflammatory cells, alveolar macrophage-derived cytokines, and histopathology. *Am J Respir Cell Mol Biol* 2: 381–390.
12. Driscoll KE, Maurer JK, Lindenschmidt RC, Romberger D, Rennard SI, Crosby L (1990) Respiratory tract responses to dust: relationships between dust burden, lung injury, alveolar macrophage fibronectin release, and the development of pulmonary fibrosis. *Toxicol Appl Pharmacol* 106: 88–101.
13. Henderson RF, Driscoll KE, Harkema JR, Lindenschmidt RC, Chang IY, Maples KR, Barr EB (1995) A comparison of the inflammatory response of the lung to inhaled versus instilled particles in F344 rats. *Fundam Appl Toxicol* 24: 183–197.
14. Warheit DB, Brock WJ, Lee KP, Webb TR, Reed KL (2005) Comparative pulmonary toxicity inhalation and instillation studies with different TiO₂ particle formulations: impact of surface treatments on particle toxicity. *Toxicol Sci* 88 (2):514–524.
15. Afaq F, Abidi P, Matin R, Rahman Q (1998) Cytotoxicity, pro-oxidant effects and antioxidant depletion in rat lung alveolar macrophages exposed to ultrafine titanium dioxide. *J Appl Toxicol* 18: 307–312.
16. Oberdörster G, Finkelstein J N, Johnston C (2000) Acute pulmonary effects of ultrafine particles in rats and mice. *Res Rep Health Eff Inst* 96: 5–74.
17. Wang J X, Zhou G Q, Chen C Y, Yu H W, Wang T C, Ma Y M, Jia G, Gao Y X, Li B, Sun J, Li Y F, Jia F, Zhao Y L, Chai Z F (2007) Acute toxicity and biodistribution of different sized titanium dioxide particles in mice after oral administration. *Toxicol Lett* 168: 176–185.
18. Liu HT, Ma L L, Zhao J F, Liu J, Yan JY, Ruan J, Hong FS (2009) Biochemical toxicity of nano-anatase TiO₂ particles in mice. *Biol Trace Element Res*, doi:10.1007/s12011-008-8285-6 (in press)
19. Yang P, Lu C, Hua N, Du Y (2002) Titanim dioxide nanoparticles co-doped with Fe³⁺ and Eu³⁺ ions for photocatalysis. *Mater Lett* 57: 794–801.
20. Wotton I D P (1964) Enzymes in blood. In *Microanalysis in Medical Biochemistry*, pp. 101–118, Churchill, London.

21. Ankudinov A, Ravel B, Rehr J J, Conradson S D (1998) Real-space multiple-scattering calculation and interpretation of x-ray-absorption near-edge structure. *Phys Rev B* 58: 7565–7576.
22. Perczel A, Park K, Fasman G D (1992) Analysis of the circular dichroism spectrum of proteins using the convex constraint algorithm: a practical guide. *Anal Biochem* 203: 83–89.
23. Chen Z, Meng H, Xing G M, Chen C Y, Zhao Y L, Jia G, Wang T C, Yuan H, Ye C, Zhao F, Chai Z F, Zhu C F, Fang X H, Ma B C, Wan L J (2006) Acute toxicological effects of copper nanoparticles in vivo. *Toxicol Lett* 163: 109–120.
24. Hong F S, Wu C, Liu C, Wang L, Gao F Q, Yang F, Xu J H, Liu T, Xie Y N, Li Z R (2007) Direct interaction between lead ions and DNA from kidney of silver crucian carp. *Chemosphere* 69: 1442–1446.
25. Nagami H, Yoshimoto N, Umakoshi H (2005) Liposome-assisted activity of superoxida dismutase under oxidative stress. *J. Biosci Bioeng* 99(4): 423–428.